International Journal of Nanomedicine

Dovepress
open access to scientific and medical research

Open Access Full Text Article

ORIGINAL RESEARCH

Magnetic nanoparticles of Fe_3O_4 enhance docetaxel-induced prostate cancer cell death

This article was published in the following Dove Press journal:
International Journal of Nanomedicine
18 August 2013

Akiko Sato[1]
Naoki Itcho[1]
Hitoshi Ishiguro[2,3]
Daiki Okamoto[1]
Naohito Kobayashi[4]
Kazuaki Kawai[5]
Hiroshi Kasai[5]
Daisuke Kurioka[1]
Hiroji Uemura[2]
Yoshinobu Kubota[2]
Masatoshi Watanabe[1]

[1]Laboratory for Medical Engineering, Division of Materials Science and Chemical Engineering, Graduate School of Engineering, Yokohama National University, Yokohama, Japan; [2]Department of Urology, Yokohama City University Graduate School of Medicine, Yokohama, Japan; [3]Photocatalyst Group, Kanagawa Academy of Science and Technology, Kawasaki, Japan; [4]Department of Molecular Pathology, Yokohama City University Graduate School of Medicine, Yokohama, Japan; [5]Department of Environmental Oncology, Institute of Industrial Ecological Sciences, University of Occupational and Environmental Health, Kitakyushu, Japan

Correspondence: Masatoshi Watanabe
Laboratory for Medical Engineering, Division of Materials Science and Chemical Engineering, Graduate School of Engineering, Yokohama National University, 79-5 Tokiwadai, Hodogayaku, Yokohama, Japan
Tel +81 453 393 997
Fax +81 453 393 997
Email mawata@ynu.ac.jp

Abstract: Docetaxel (DTX) is one of the most important anticancer drugs; however, the severity of its adverse effects detracts from its practical use in the clinic. Magnetic nanoparticles of Fe_3O_4 (MgNPs-Fe_3O_4) can enhance the delivery and efficacy of anticancer drugs. We investigated the effects of MgNPs-Fe_3O_4 or DTX alone, and in combination with prostate cancer cell growth in vitro, as well as with the mechanism underlying the cytotoxic effects. MgNPs-Fe_3O_4 caused dose-dependent increases in reactive oxygen species levels in DU145, PC-3, and LNCaP cells; 8-hydroxydeoxyguanosine levels were also elevated. MgNPs-Fe_3O_4 alone reduced the viability of LNCaP and PC-3 cells; however, MgNPs-Fe_3O_4 enhanced the cytotoxic effect of a low dose of DTX in all three cell lines. MgNPs-Fe_3O_4 also augmented the percentage of DU145 cells undergoing apoptosis following treatment with low dose DTX. Expression of nuclear transcription factor κB in DU145 was not affected by MgNPs-Fe_3O_4 or DTX alone; however, combined treatment suppressed nuclear transcription factor κB expression. These findings offer the possibility that MgNPs-Fe_3O_4–low dose DTX combination therapy may be effective in treating prostate cancer with limited adverse effects.
Keywords: prostate cancer, magnetic nanoparticles, docetaxel, reactive oxidative species

Introduction

Prostate cancer is the most common cancer affecting men, and the second leading cause of cancer death in the United States.[1] The incidence and mortality rates of prostate cancer vary greatly among different geographic areas and ethnic groups. Although the incidence of prostate cancer in Japan remains low compared with that in the United States, it has been increasing in recent years. However, by 2020, prostate cancer is projected to surpass stomach cancer as the most frequently diagnosed cancer in Japanese men.[2]

Several management options are available when prostate cancer is diagnosed at an early stage, including watchful waiting, surgery, cryosurgery, radiation therapy, and hormonal therapy. For advanced prostate cancers, surgical or medical ablation of androgens is regarded the optimal first-line treatment. In most patients treated by androgen deprivation, disease progression will continue until reaching a stage referred to as castration-resistant prostate cancer (CRPC). Progression to a hormonal refractory state is a complex process, involving both selection and outgrowth of preexisting clones of androgen-independent cells as well as adaptive upregulation of genes that help cancer cells survive and grow after androgen ablation.[3]

Although the effects of several anticancer drugs for prostate cancer have been evaluated in vitro and in animal experiments in vivo, most have little or no impact on the survival of patients with CRPC or metastatic prostate cancer.[4,5] Docetaxel (DTX), a semisynthetic toxoid produced from the needles of the European yew tree, is the first chemotherapy agent to improve survival in CRPC, and the US Food and Drug Administration has recommended a 3-week DTX-prednisone regimen as a first-line treatment option for CRPC patients.[6–8] Although DTX-based chemotherapy may provide some benefits, most CRPC patients do not realize them, and the average survival remains relatively brief. Moreover, the current regimen requires the administration of high doses of DTX, which causes toxic reactions and thereby precludes the use of DTX as a monotherapy.[9] To reduce toxicity and to improve the survival and quality of life of CRPC patients, novel therapeutic strategies targeting the molecular basis of androgen- and chemo-resistance of prostate cancer using a reduced but equieffective dose of DTX should be developed.

Cancer nanotechnology offers great potential for cancer diagnosis, targeted treatment, and monitoring.[10] Researchers are exploring the use of nanoparticles (NPs) ranging in length from 1 nm to 100 nm in two or three dimensions to detect, image, monitor, and treat cancers. Among the rapidly evolving types of NPs, magnetic NPs (MgNPs) – biocompatible and superparamagnetic nanomaterials with chemical stability and low toxicity – are especially promising.[11] The combination of MgNPs with anticancer agents has been applied to leukemia, lung, and pancreatic cancer cells in vitro and to xenograft-injected nude mice.[12–15] MgNPs composed of Fe_3O_4 (MgNPs-Fe_3O_4) are being widely investigated for use as targeted drug carriers. The aim of this study was to evaluate the effect of treatment with MgNPs-Fe_3O_4 or MgNPs-Fe_3O_4 combined with DTX on prostate cancer cell growth in vitro. We also explored the mechanism underlying MgNPs-Fe_3O_4-induced cell death, focusing on the effect of MgNPs-Fe_3O_4 treatment on the production of reactive oxygen species (ROS).

Materials and methods

Physical characterization of MgNPs-Fe_3O_4

MgNPs-Fe_3O_4 were obtained from the Toda Kogyo Corporation (Otake, Hiroshima, Japan) and had the following characteristics: spherical shape; an average particle size of 10 nm in powder and 8–10 nm as measured by transmission electron microscopy (TEM); a size of 60–100 nm as measured by dynamic light scattering (DLS); a zeta potential of –30 to –40 mV at a pH of 10; and a surface area in powder of 100–120 m^2/g.

Preparation of MgNPs-Fe_3O_4

After ultraviolet sterilization of the particles, MgNPs-Fe_3O_4 stocks were prepared by suspending particles in Roswell Park Memorial Institute (RPMI)-1640 with supplements to yield final concentrations of 1 μg/mL, 10 μg/mL, or 100 μg/mL, followed by sonication at 30 W for 10 minutes with an Ultrasonic Homogenizer VP-050 (TAITEC, Koshigaya, Saitama, Japan).

Docetaxel

DTX was purchased from Sigma-Aldrich (St Louis, MO, USA) and dissolved in dimethyl sulfoxide (DMSO; stock solution). Stock solutions were aliquoted and stored at –20°C to avoid repetitive freeze–thaw cycles. Stock solutions were serially diluted using culture medium to prepare working solutions.

Cell lines

LNCaP, DU145, and PC-3 human prostate cancer cell lines were purchased from American Tissue Type Culture Collection (Manassas, VA, USA). Cells were cultured in RPMI-1640 medium with 10% fetal bovine serum (FBS) and 100 U/mL penicillin–streptomycin in 5% CO_2 at 37°C. The human normal prostate stromal cell (PrSC) line was obtained from BioWhittaker® (Lonza Walkersville, Inc, Walkersville, MD, USA) and maintained in Dulbecco's modified Eagle's medium supplemented with 10% FBS, 100 U/mL of penicillin G, 100 μg/mL of streptomycin, ITH (5 μg/mL insulin, 5 μg/mL transferrin, and 1.4 μmol/L hydrocortisone), and 5 ng/mL of bFGF in 5% CO_2 at 37°C.

Characterization of MgNPs-Fe_3O_4 suspension

MgNP-Fe_3O_4 suspensions and their cellular localization were characterized using the following methods.

Dynamic light scattering (DLS)

The average hydrodynamic size and size distribution of MgNPs-Fe_3O_4 in media were determined by DLS using a Fiber-Optics Particle Analyzer FPAR-1000 (Otsuka Electronics Co, Ltd, Hirakata, Osaka, Japan). DU145 cells were incubated with MgNPs-Fe_3O_4 (1 μg/mL, 10 μg/mL, or 100 μg/mL).

Transmission electron microscopy (TEM)

DU145 cells were incubated with MgNPs-Fe_3O_4 (10 μg/mL). After incubation for 24 hours, cells were collected, washed three times with phosphate buffered saline (PBS), and fixed with 3% glutaraldehyde in 0.1 M cacodylate buffer (pH 7.3) at 4°C for 4 hours. The resulting samples were postfixed with 2% osmium tetraoxide at 4°C for 2 hours, dehydrated, and embedded in epoxy resin. Ultrathin sections (80 nm) were then stained with uranyl acetate and lead citrate, and observed by TEM.

Measurement of intracellular reactive oxygen species

ROS were measured using the CM-H2DCFDA assay (Life Technologies, Carlsbad, CA, USA), according to the manufacturer's instructions. DU145 cells (1.0×10^5 cells/well) were incubated with MgNPs-Fe_3O_4 (1 μg/mL, 10 μg/mL, or 100 μg/mL) for 24 hours in the absence or presence of N-acetylcysteine (NAC; 10 mM) (Sigma-Aldrich Co); NAC was added 3 hours before treatment with MgNPs-Fe_3O_4. A stock solution of CM-H2DCFDA (5 mM) was freshly prepared in DMSO and diluted to a final concentration of 1 μM in PBS. Cells were washed with PBS followed by incubation with 50 μL of working solution of fluorochrome marker CM-H2 DCFDA for 30 minutes. Fluorescent imaging was recorded using an IX2 N-FL-1 microscope (Olympus Corporation, Tokyo, Japan), and analyzed using imaging software (Adobe Photoshop Elements 8; Adobe Systems Incorporated, San Jose, CA, USA). As a positive control, cells were treated with H_2O_2 (100 μM) for 24 hours.

Analysis of 8-hydroxydeoxyguanosine in DNA

The MgNPs-Fe_3O_4 (1 μg/mL, 10 μg/mL, or 100 μg/mL) were added to wells containing DU145, PC-3, or LNCap cells (5.0×10^6 cells), and incubated for 72 hours at 37°C (5% CO_2). Nuclear deoxyribonucleic acid (DNA) of the cells was isolated by the sodium iodide method. Analysis of 8-hydroxydeoxyguanosine (8-OH-dG) was performed as previously described.[16] The 8-OH-dG levels were measured by high performance liquid chromatography electrochemical detection. The amount of 8-OH-dG in the DNA was determined through comparisons with the authentic standards, and expressed as the number of 8-OH-dG per 10^6 deoxyguanosine (dG).

AlamarBlue® assay

Cell viability was determined using the AlamarBlue® assay (Alamar Biosciences, Inc, Sacramento, CA, USA), according to the manufacturer's instructions. Briefly, cells were seeded in 24-well plates (1.0×10^4 cells/well); cells were treated with DTX (0.1 μM, 1 μM, 10 μM, or 100 μM) or DTX (1 nM) plus MgNPs-Fe_3O_4 (1 μg/mL, 10 μg/mL, or 100 μg/mL) for 48 hours at 37°C (5% CO_2). AlamarBlue® was added to each well at 10% volume and was incubated for 200 minutes. Metabolically active cells reduced the dye into a fluorescent form; fluorescence intensity was measured using a plate reader (excitation/emission: 570 nm/600 nm; Viento XS, DS Pharma Biomedical Co, Ltd, Suita, Osaka, Japan). Fluorescence intensity was used to estimate cell viability by linear interpolation between the emission from cells treated with 0.1% saponin (0% viability) and that from untreated cells (100% viability).

Flow cytometry (FCM) analysis for cell apoptosis

The apoptotic peak (sub-G1) of cells was measured using FCM. DU145 cells (1.0×10^6 cells) were seeded in 100 mm culture dishes; cells were either untreated (control), or treated with DTX (1 nM) or MgNPs-Fe_3O_4 (10 μg/mL or 100 μg/mL) in the absence or presence of DTX (1 nM). Aspirated medium was collected to determine the amount of floating cells and cell debris as indicators of cell death. Cells were collected and fixed in ice-cold 70% ethanol and stored at –20°C before use. In preparation for use, cells were washed with PBS and resuspended in PBS before incubation with ribonuclease (0.5 mg/mL) at room temperature for 30 minutes. After the addition of 1 mg/mL of propidium iodide (PI; Sigma-Aldrich), the cells were passed through a 40 mm nylon mesh for analysis using an LSRII flow cytometer (BD Bioscience Franklin Lakes, NJ, USA). The fluorescence intensities of PI were measured by FCM, and the number of cells in the sub-G1 peak was determined. Quantification of the fraction was performed with ModFit LT for Mac 3.0 (Verity Software House, Topsham, ME, USA).

Annexin-V assay was used to detect the early phases of apoptosis. Apoptosis was assessed by monitoring the expression of phosphatidylserine on the outer leaflet – an early marker of apoptotic cell death. Phosphatidylserine was stained with fluorescein isothiocyanate (FITC)-labeled Annexin V. Loss of membrane integrity as a consequence of necrosis was detected using PI staining of DNA. Briefly, DU145 cells (1.0×10^6) were either untreated (control) or treated with DTX (1 nM), or with MgNPs-Fe_3O_4 (10 μg/mL or 100 μg/mL) for 24 hours in the absence or presence of DTX (1 nM). After incubation, cells were harvested, gently washed twice in ice-cold PBS, collected by centrifugation, and then stained using an Annexin V-FITC Kit (Beckman Coulter, Inc, Fullerton, CA, USA) according to the manufacturer's instructions. Cells were then stained with Annexin V and PI for analysis by FCM within 1 hour of staining using the FL1 (FITC) and FL3 (PI) lines.

Western blot analysis

Cells were lysed in Radioimmunoprecipitation assay buffer (Sigma-Aldrich) containing protease inhibitors (Sigma-Aldrich). Total protein concentration was determined by Bio-Rad protein assay reagent (Bio-Rad Laboratories, Hercules, CA, USA). Equal amounts of lysates were resolved on sodium dodecyl sulfate-polyacrylamide gel electrophoresis and transferred to a polyvinylidene fluoride membrane (Merck Millipore, Billerica, MA, USA). Membranes were blocked with a blocking reagent (NOF Corporation, Tokyo, Japan) for 1 hour at room temperature, and incubated overnight at 4°C with the respective primary antibodies in Tris-buffered saline and Tween 20 (TBST). The membranes were washed with TBST three times and incubated with diluted horseradish peroxidase-conjugated secondary antibodies (1:3000 for nuclear factor κB [NFκB]; 1:10,000 for β-actin) for 1 hour at room temperature. After three additional washes, membranes were detected using an enhanced chemiluminescence kit (GE Healthcare UK Ltd, Little Chalfont, UK). Antibodies against NFκB and β-actin were purchased from Santa Cruz Biotechnology, Inc (Santa Cruz, CA, USA) and Sigma-Aldrich, respectively; antirabbit and antimouse horseradish peroxidase-conjugated secondary antibodies were purchased from GE Healthcare (GE Healthcare UK Ltd).

Statistical analysis

All experiments were repeated at least three times. Data are represented as the mean ± standard deviation. Data were analyzed using an unpaired Student's t-test with or without Welch's correction and ANOVA. Differences were considered statistically significant at $P < 0.05$.

Results

MgNPs-Fe_3O_4 characterization in cell culture medium

Figure 1 shows the mean hydrodynamic diameter of MgNPs-Fe_3O_4 in medium with supplements as measured by DLS. The mean hydrodynamic diameter of MgNPs-Fe_3O_4 increased with increasing concentration, suggesting that aggregation is enhanced at higher concentrations.

Cellular uptake

Cellular uptake of MgNPs-Fe_3O_4 was evident from TEM microphotographs (Figure 2). MgNPs-Fe_3O_4 were localized within intracellular vesicles.

ROS production

MgNPs-Fe_3O_4 caused dose-dependent increases of ROS production in DU145 and PC-3 cells; a significant increase in LNCaP cells was evident only at the highest dose. Treatment with 100 μg/mL of MgNPs-Fe_3O_4 elicited a

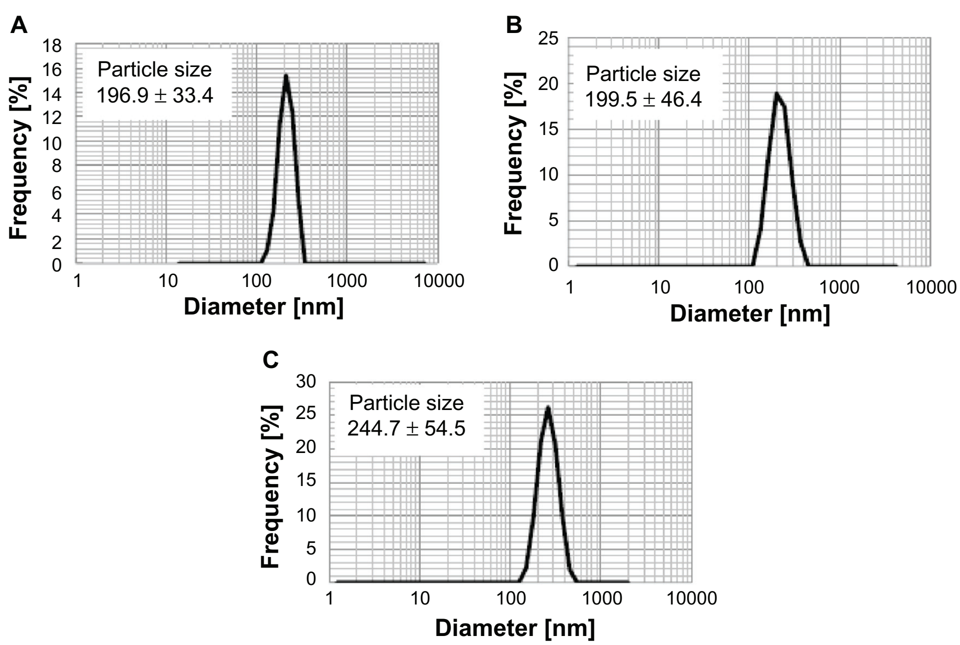

Figure 1 Measurement of MgNPs-Fe_3O_4 size by dynamic light scattering. DU145 cells were incubated with MgNPs-Fe_3O_4: (**A**) 1 μg/mL, (**B**) 10 μg/mL, and (**C**) 100 μg/mL.
Abbreviation: MgNPs-Fe_3O_4, Fe_3O_4 magnetic nanoparticles.

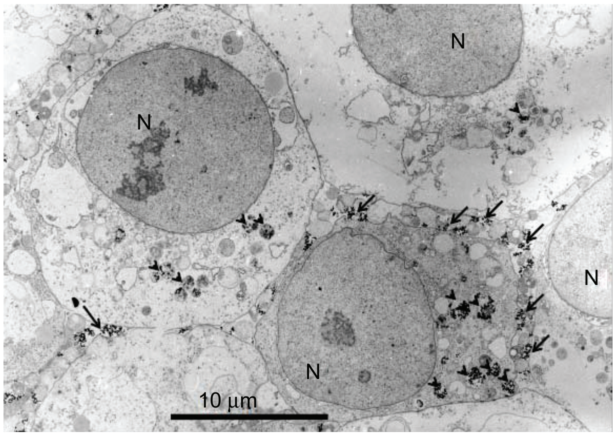

Figure 2 Transmission electron microscopy imaging of DU145 cells treated with 10 µg/mL of Fe_3O_4 magnetic nanoparticles.
Notes: Arrow: extracellular magnetic nanoparticles; arrow head: intracellular magnetic nanoparticles.
Abbreviation: N, nucleus.

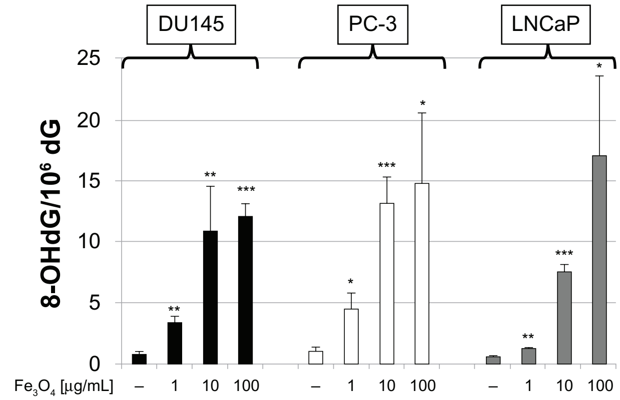

Figure 4 8-OH-dG levels in DU145, PC-3, and LNCaP cells after 72 hours of treatment with MgNPs-Fe_3O_4.
Notes: Data are presented as the mean ± SD of three independent experiments. *Significantly different from the untreated control at $P < 0.05$; **significantly different from the control at $P < 0.01$; ***significantly different from the untreated control at $P < 0.001$.
Abbreviations: 8-OH-dG, 8-hydroxydeoxyguanosine; MgNPs-Fe_3O_4, Fe_3O_4 magnetic nanoparticles; SD, standard deviation.

response comparable to that evoked by H_2O_2 (Figure 3). Among the three cell lines, ROS levels in the DU145 and PC-3 lines were higher than that in the LNCaP line. Pretreatment with NAC attenuated the MgNPs-Fe_3O_4-induced rise in ROS in all three prostate cancer cell lines (Figure 3).

8-OH-dG levels in DNA

The 8-OH-dG levels in the DNA in all three prostate cancer cell lines increased in a dose-dependent manner (Figure 4). The 8-OH-dG levels of DU145 and PC-3 cells exposed to 10 µg/mL of MgNPs-Fe_3O_4 were 13-fold to 14-fold greater than that of the untreated control cells.

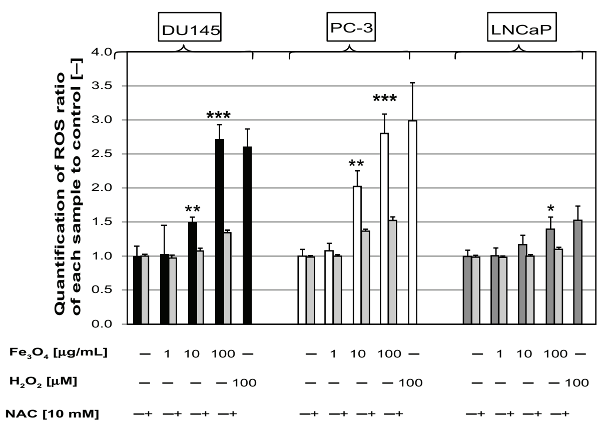

Figure 3 Production of intracellular ROS in DU145, PC-3, and LNCaP cells after treatment with MgNPs-Fe_3O_4 for 24 hours in the absence or presence of NAC.
Notes: Data are presented as the mean ± SD of three independent experiments. *Significantly different from the untreated control at $P < 0.05$; **significantly different from the control at $P < 0.01$; ***significantly different from the untreated control at $P < 0.001$.
Abbreviations: ROS, reactive oxygen species; MgNPs-Fe_3O_4, Fe_3O_4 magnetic nanoparticles; NAC, N-acetylcysteine; SD, standard deviation.

Effect of MgNPs-Fe_3O_4, DTX, and MgNPs-Fe_3O_4–DTX combinations on cell viability

MgNPs-Fe_3O_4 alone reduced the viability of LNCaP and PC-3 cells, but had little or no effect on the viability of DU145 and PrSC cells (Figure 5). These results suggest that the cytotoxicity of MgNPs-Fe_3O_4 may be dependent on the cell type of the prostate cancer cell line. DTX alone decreased cell viability in a dose-dependent manner in all three cancer cell lines (Figure 6). Combined treatment with MgNPs-Fe_3O_4 and DTX enhanced the inhibitory effect of DTX; in PC-3 cells, 100 µg/mL of MgNPs-Fe_3O_4 plus 1 nM of DTX reduced cell viability so it was similar to that caused by 10 nM DTX alone. These data suggest that MgNPs-Fe_3O_4 may be beneficial in reducing the DTX dose it may and thereby overcome the safety limitations of DTX.

Effect of MgNPs-Fe_3O_4, DTX, and MgNPs-Fe_3O_4–DTX combinations on cell death

An apoptotic fraction of cells containing subdiploid amounts of DNA was detected as a sub-G1 peak (Figure 7). MgNPs-Fe_3O_4 caused a dose-dependent increase in the percentage of DU145 cells in the sub-G1 fraction; similarly, DTX alone elicited a rise in the percentage of cells in the sub-G1 fraction. Combined treatment with MgNPs-Fe_3O_4 plus DTX augmented the effect compared to either treatment alone; this enhancement was dose-dependent.

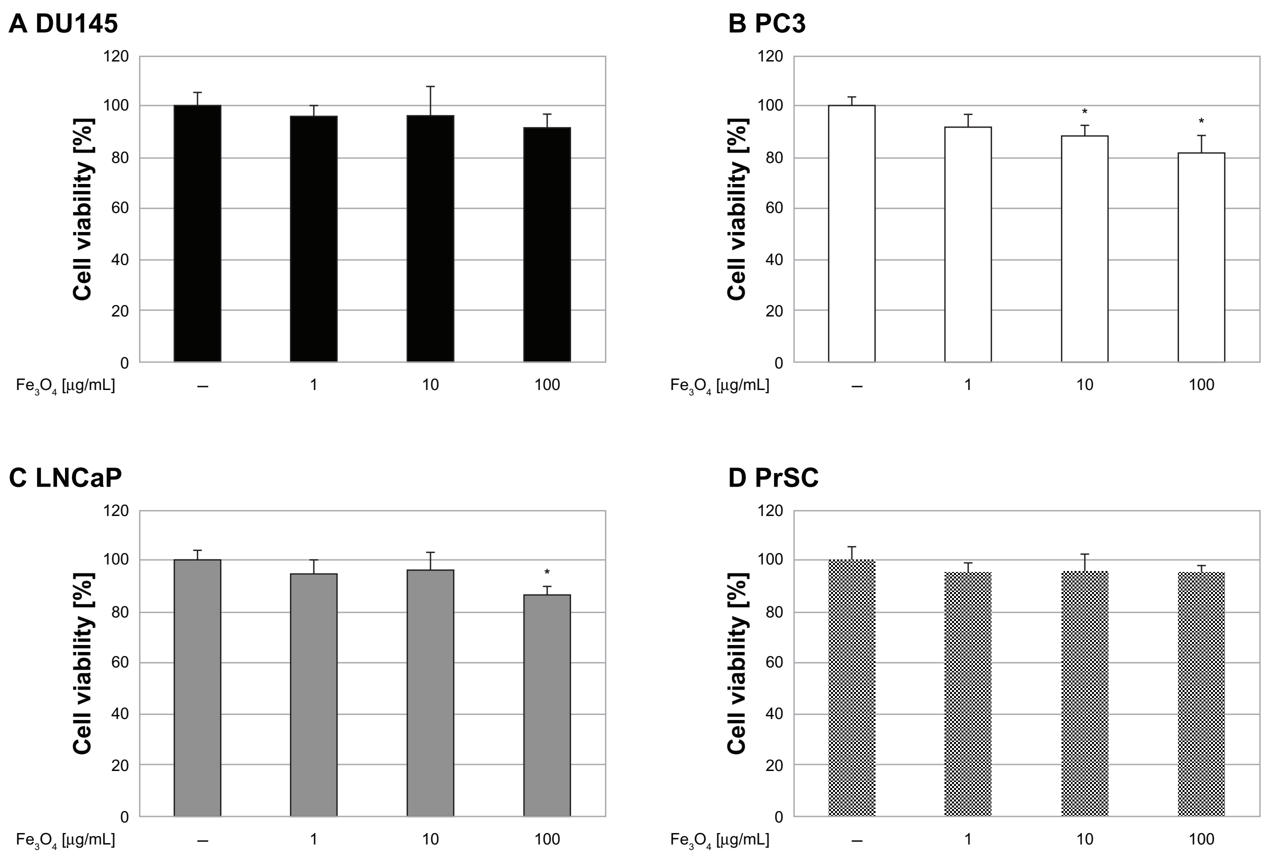

Figure 5 Effect of MgNPs-Fe_3O_4 exposure on cell line viability. Effect of MgNPs-Fe_3O_4 exposure on the viability of (**A**) DU145, (**B**) PC-3, (**C**) LNCaP, and (**D**) PrSC cell lines.
Notes: Data are presented as the mean ± SD of three independent experiments. *Significantly different from the control at $P < 0.05$.
Abbreviations: MgNPs-Fe_3O_4, Fe_3O_4 magnetic nanoparticles; SD, standard deviation.

Neither MgNPs-Fe_3O_4 nor DTX alone increased Annexin V/PI staining (Figure 8). Conversely, a significant increase in the percentage of apoptotic cells was observed during the combined treatment with NPs-Fe_3O_4 and DTX compared to the untreatment, the treatment with MgNPs-Fe_3O_4 alone, or DTX alone ($P < 0.05$).

Effect of MgNPs-Fe_3O_4 and MgNPs-Fe_3O_4–DTX combinations on NFκB expression in DU145 cells

Treatment with MgNPs-Fe_3O_4 alone did not lower NFκB expression in DU145 cells; conversely, treatment with MgNPs-Fe_3O_4–DTX combinations inhibited NFκB expression in a dose-dependent manner (Figure 9).

Discussion

DTX remains the cornerstone of chemotherapy for treating prostate cancer when castration resistance is documented and secondary hormone therapy is ineffective. However, to be effective, DTX must be administered at such high doses that can induce significant toxicity.[9,17] To overcome this drawback, combination therapies have been developed; DTX combined with tyrosine kinase or bcl-2 inhibitors are currently in Phase II studies for treating CRPC.[17] Drug-delivery assemblies consisting of a nanocarrier, a targeting agent, and DTX have also been developed. For example, NC-6301 – a polymeric micelle with DTX – shows less toxicity than native DTX in vivo; NC-6301 is a nanoscale drug delivery system approximately 100 nm in a diameter.[18] In the present study, we found that DTX alone has a strong anticancer effect, and the cytotoxic effect of a low concentration (1 nM) is augmented by MgNPs-Fe_3O_4.

Many studies have focused on the use of NPs, especially MgNPs, in theranostics.[10,11] Due to their biocompatibility and stability, iron oxide MgNPs, particularly magnetic Fe_3O_4 and its oxidized and more stable form, maghemite γ-Fe_2O_3, are superior for biomedical applications compared to other metal oxide NPs. Moreover, iron oxide NPs may have additional utility as a contrast agent in magnetic resonance imaging or as a carrier for drug delivery.[11–15] In the present study, we focused on MgNPs-Fe_3O_4 because of their potential to treat CRPC. This stems from the intrinsic properties of the magnetic core combined with the drug

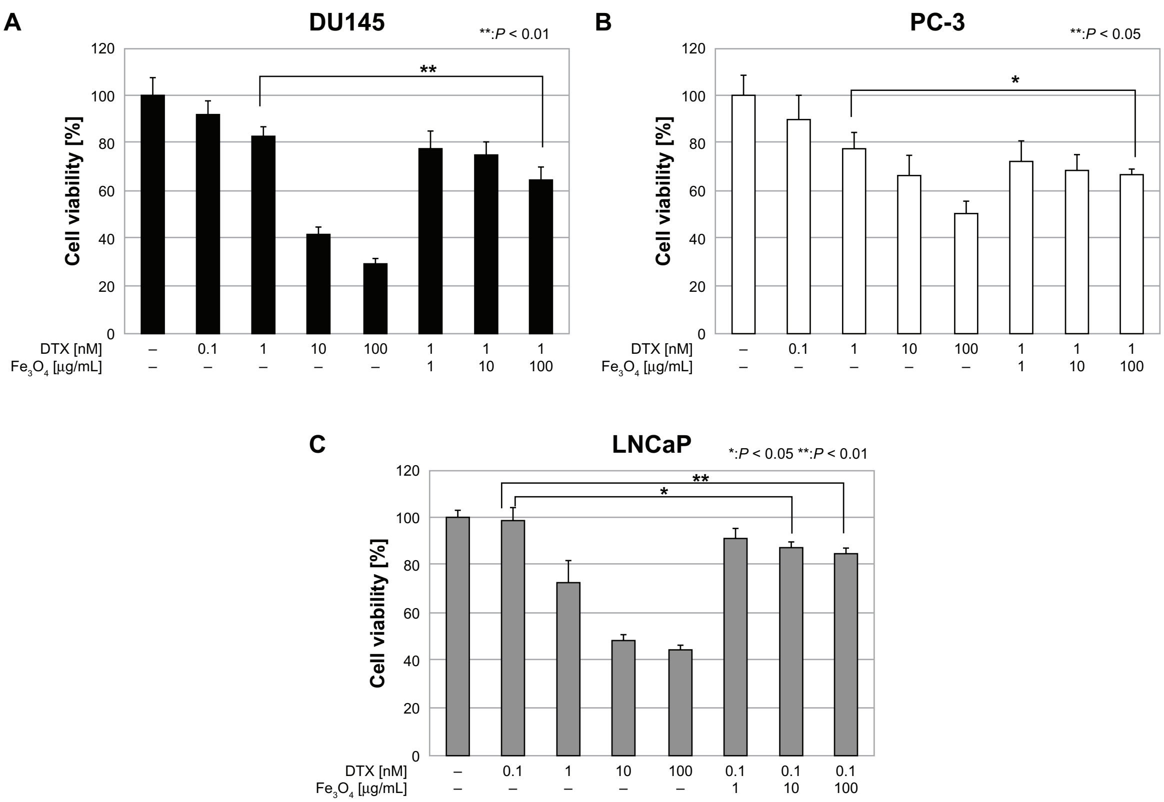

Figure 6 Effect of DTX alone or in combination with MgNPs-Fe_3O_4 on cell viability. Effect of DTX alone or in combination with MgNPs-Fe_3O_4 on the viability of (**A**) DU145, (**B**) PC-3, and (**C**) LNCaP cell lines.

Notes: Data are presented as the mean ± SD of three independent experiments. *Significantly different from the control at $P < 0.05$; **significantly different from the control at $P < 0.01$.

Abbreviations: DTX, docetaxel; MgNPs-Fe_3O_4, Fe_3O_4 magnetic nanoparticles; SD, standard deviation.

loading capability and the biomedical properties of MgNPs conferred by different surface coatings. Iron oxide MgNPs have also effectively been used in combination with chemotherapy and hyperthermia to overcome drug resistance in a leukemia xenograft model,[19] and with doxorubicin under a static magnetic field to enhance the doxorubicin-mediated cytotoxicity of MCF-7 cells.[20]

Results from several studies suggest that the cytotoxic effects of MgNPs are dependent on the metal and target cell type.[21,22] CuO, ZnO, and $CuZnFe_2O_4$, but not Fe_2O_3 or

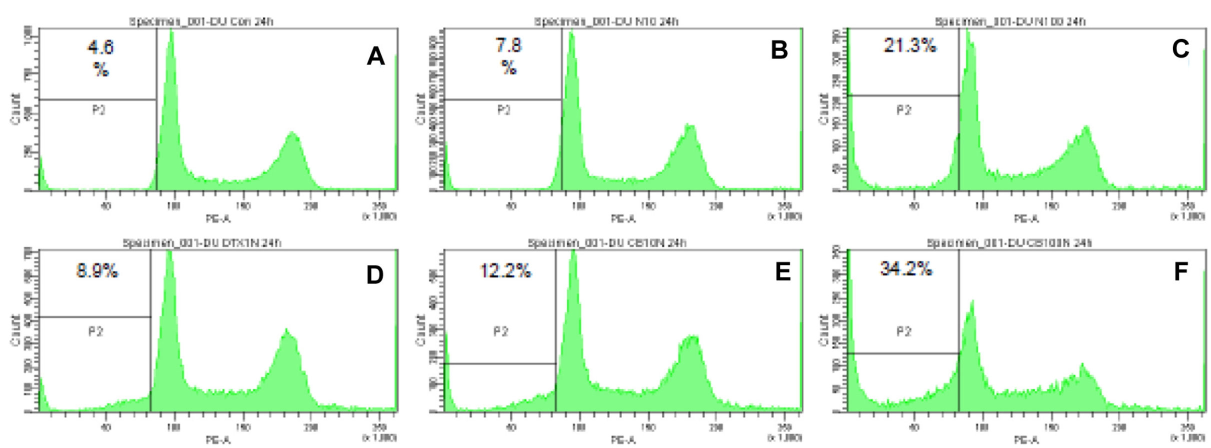

Figure 7 Flow cytometry analysis of apoptosis of DU145 cells. Panels represent the following treatments: (**A**) untreated (control); (**B**) MgNPs-Fe_3O_4 (10 µg/mL); (**C**) MgNPs-Fe_3O_4 (100 µg/mL); (**D**) DTX (1 nM); (**E**) DTX (1 nM) + MgNPs-Fe_3O_4 (10 µg/mL); and (**F**) DTX (1 nM) + MgNPs-Fe_3O_4 (100 µg/mL).

Notes: Cells were incubated with each condition for 24 hours. The percentage of cells in the sub-G1 phase was quantified for each plot.

Abbreviations: MgNPs-Fe_3O_4, Fe_3O_4 magnetic nanoparticles; DTX, docetaxel.

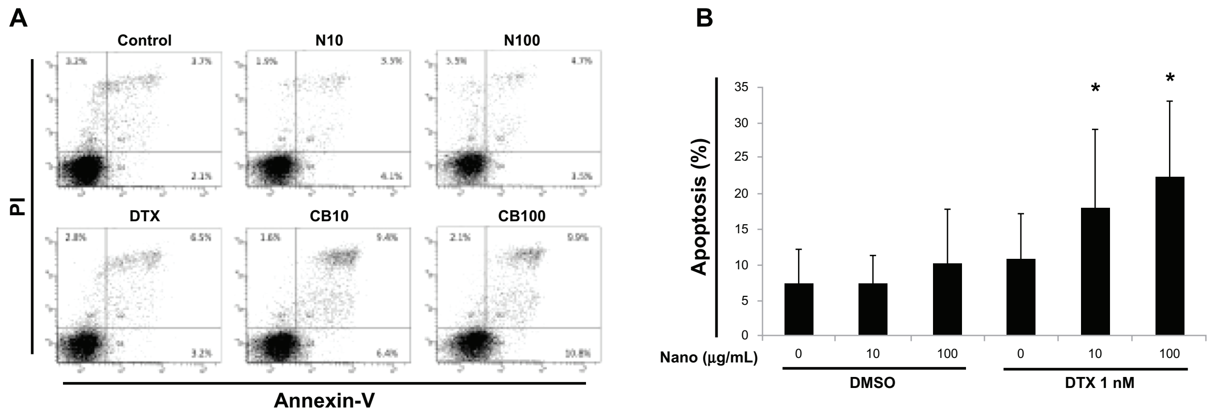

Figure 8 Effects of MgNPs-Fe_3O_4 and docetaxel (DTX) alone or in combination on apoptosis in DU145 cells. (**A**) Representative FCM using Annexin V/PI staining of one set of triplicate experiments. N10: MgNPs-Fe_3O_4 (10 μg/mL); N100: MgNPs-Fe_3O_4 (100 μg/mL); DTX: DTX (1 nM); CB10: DTX (1 nM) + MgNPs-Fe_3O_4 (10 μg/mL); and CB100: DTX (1 nM) + MgNPs-Fe_3O_4 (100 μg/mL). (**B**) Percentages of apoptotic cells from FCM analysis.

Notes: Data are presented as the mean ± SD of three independent experiments. Results show that the combination of 10 μg/mL or 100 μg/mL of MgNPs-Fe_3O_4 with 1 nM of DTX induced significant apoptosis in DU145 cells compared to untreated cells, cells treated with 10 μg/mL or 100 μg/mL of MgNPs-Fe_3O_4 alone, or 1nM of DTX alone (*$P < 0.05$).

Abbreviations: MgNPs-Fe_3O_4, Fe_3O_4 magnetic nanoparticles; DTX, docetaxel; PI, propidium iodide; DMSO, dimethyl sulfoxide; FCM, flow cytometry analysis; SD, standard deviation.

Fe_3O_4, were highly toxic to the human lung epithelial cell line A549; CuO NPs were especially effective in inducing a significant increase in ROS production.[21] In BRL 3A liver cells, only silver NPs were highly toxic; Fe_3O_4, tungsten, aluminum, and MnO_2 exhibited little or no toxicity.[23] Conversely, iron oxide MgNPs caused hepatic and renal damage when administered to mice,[22] and the reduced viability of J774 macrophages in vitro.[24]

ROS act as a second messenger in cell signaling and are involved in various biological processes, such as growth and survival in normal cells. Oxidative stress reflects a redox imbalance within the cells and usually results from

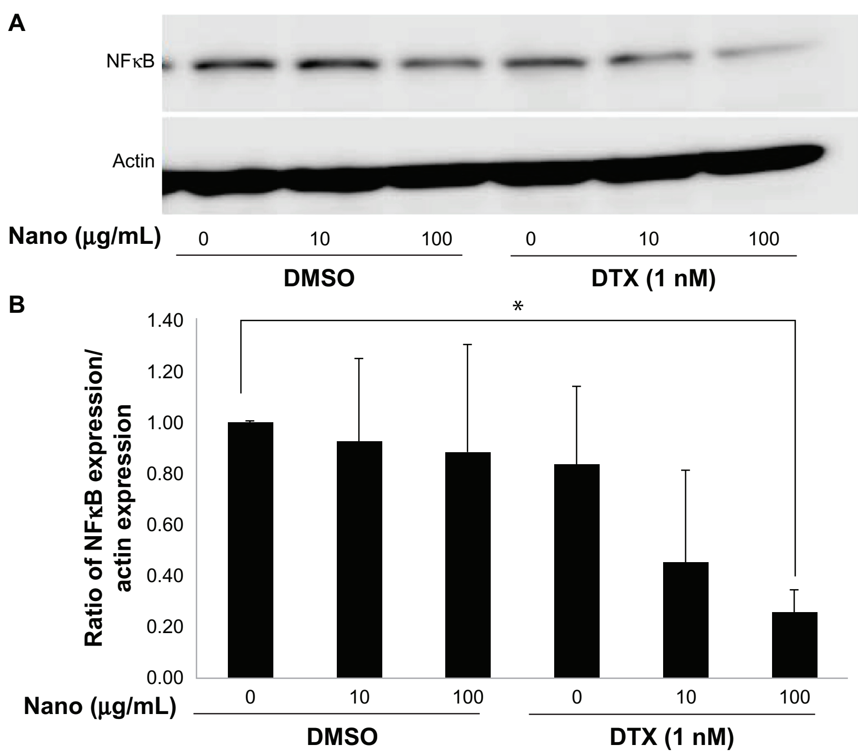

Figure 9 Effects of MgNPs-Fe_3O_4 in the absence or presence of DTX on NFκB expression in DU145 cells. (**A**) Western blot analysis. (**B**) Densitometric analysis of NFkB/actin expression ratio.

Notes: Cells were treated for 48 hours. The ratio of NFκB expression/actin expression represents the mean ± SD of three independent experiments. Results show that NFkB expression decreased in DU145 cells treated with 100 μg/mL of MgNPs-Fe_3O_4 with 1 nM of DTX compared to untreated cells (*$P < 0.05$).

Abbreviations: MgNPs-Fe_3O_4, Fe_3O_4 magnetic nanoparticles; DMSO, dimethyl sulfoxide; DTX, docetaxel; NFκB, nuclear factor κB; SD, standard deviation.

the net accumulation of intracellular ROS, which are not detoxified by cellular antioxidative agents.[25] In cancer cells, the production of ROS is typically increased; since they play important roles in initiation, progression, and metastasis, ROS are considered oncogenic. However, ROS are also implicated in triggering cell death, including that of cancer cells; thus, their production is desirable in chemotherapy, radiotherapy, and photodynamic therapy. This dual role of ROS has led to the development of two paradoxical ROS-manipulation strategies in cancer treatment.[25] One strategy is to treat tumor cells with antioxidants, such as through the dietary administration of red wine and green tea polyphenols to prevent cancer. The other strategy is to provide pro-oxidant therapy, which consists of generating ROS directly and inhibiting antioxidative enzyme systems in tumor cells. In the present study, MgNPs-Fe_3O_4 exhibited mild cytotoxicity toward PC-3 and LNCaP, but not toward DU145 and PrSC cells. The LNCaP and PC-3 cell lines have previously been reported to have unique redox state properties, including the production of different levels of oxidative damage products and antioxidant proteins; these differences may provide new insights into the possible uses and dangers of using pro-oxidants or antioxidants as cancer therapeutic agents.[26–28] We found that the MgNPs-Fe_3O_4-induced increase in ROS was most robust in the DU145 and PC-3 cell lines; however, the levels of 8-OH-dG, an index of oxidative DNA damage, were comparably elevated in all three cell lines.

The transcription of antiapoptotic genes is activated by the NFκB signaling pathway, resulting in cell survival. The NFκB signaling pathway also plays a critical role in cancer development and progression, and in the development of tumor resistance to chemotherapy and radiation therapy,[29] particularly in the transition toward CRPC.[30] Previous studies demonstrating a relationship between elevated NFκB and a worse prognosis support this notion.[31,32] Thus, the NFκB pathway has become an important target in the development of novel anticancer treatments. The combination of magnetic NPs with either adriamycin or daunorubicin has been reported to increase p53 levels and decrease NFκB protein levels, leading to increased apoptosis in Raji lymphoma cells.[33] In the present study, treatment with MgNPs-Fe_3O_4 or DTX alone had no effect on the expression of NFκB in DU145 cells; however, treatment with MgNPs-Fe_3O_4–DTX combinations decreased expression in a dose-dependent manner. This result is unique because many NPs have been reported to activate the NFκB pathway via activation of mitogen-activated protein kinase cascades by an oxidative stress response.[34] Thus, our results suggest that the decrease in NFκB expression resulting from treatment with MgNPs-Fe_3O_4–DTX combinations may be uncoupled from ROS generation. Although the chemical components involved in NFκB inhibition and ROS production have been identified, the contribution of MgNPs-Fe_3O_4 exposure to the mechanisms of induction and action remains unclear. Further studies such as those measuring NFκB DNA-binding activity are needed.

Conclusion

We found that MgNPs-Fe_3O_4 significantly increased ROS production in prostate cancer cell lines and induced oxidative DNA damage; the cytotoxic effects of MgNPs-Fe_3O_4 alone were mild. Treatment with a combination of MgNPs-Fe_3O_4 and a low dose of DTX enhanced the inhibitory effect of DTX alone on prostate cancer cell growth in vitro, and also suppressed NFκB expression. These findings offer the possibility that MgNPs-Fe_3O_4 may allow the dose of DTX to be reduced without decreasing its antitumor activity.

Acknowledgments

We thank Dr T Yabana for TEM analysis, and Dr M Yoneda for his pathological preparation. This research was supported in part by a Grant-in-Aid for the Global COE Program from the Ministry of Education, Culture, Sports, Science and Technology of Japan, a Grant-in-Aid for Research on Risk of Chemical Substances from the Ministry of Health, Labor and Welfare of Japan, and a Research Grant-in-Aid from Magnetic Health Science Foundation.

Disclosure

The authors report no conflicts of interest in this work. The authors have no financial interests in or financial conflict with the subject matter discussed in this manuscript.

References

1. Jemal A, Siegel R, Xu J, Ward E. Cancer statistics, 2010. *CA Cancer J Clin*. 2010;60(5):277–300.
2. Tabata N, Ohno Y, Matsui R, et al. Partial cancer prevalence in Japan up to 2020: estimates based on incidence and survival data from population-based cancer registries. *Jpn J Clin Oncol*. 2008;38(2):146–157.
3. So A, Gleave M, Hurtado-Col A, Nelson C. Mechanisms of the development of androgen independence in prostate cancer. *World J Urol*. 2005;23(1):1–9.
4. Diaz M, Patterson SG. Management of androgen-independent prostate cancer. *Cancer Control*. 2004;11(6):364–373.
5. Lassi K, Dawson NA. Update on castrate-resistant prostate cancer: 2010. *Curr Opin Oncol*. 2010;22(3):263–267.
6. Tannock IF, de Wit R, Berry WR, et al; for TAX 327 Investigators. Docetaxel plus prednisone or mitoxantrone plus prednisone for advanced prostate cancer. *N Engl J Med*. 2004;351(15):1502–1512.

7. Petrylak DP, Tangen CM, Hussain MH, et al. Docetaxel and estramustine compared with mitoxantrone and prednisone for advanced refractory prostate cancer. *N Engl J Med*. 2004;351(15):1513–1520.
8. Niraula S, Tannock IF. Broadening horizons in medical management of prostate cancer. *Acta Oncol*. 2011;50 Suppl 1:141–147.
9. Lee SY, Cho JS, Yuk DY, et al. Obovatol enhances docetaxel-induced prostate and colon cancer cell death through inactivation of nuclear transcription factor-kappaB. *J Pharmacol Sci*. 2009;111(2):124–136.
10. Misra R, Acharya S, Sahoo SK. Cancer nanotechnology: application of nanotechnology in cancer therapy. *Drug Discov Today*. 2010; 15(19–20):842–850.
11. Shubayev VI, Pisanic TR 2nd, Jin S. Magnetic nanoparticles for theragnostics. *Adv Drug Deliv Rev*. 2009;61(6):467–477.
12. Cheng J, Wu W, Chen BA, et al. Effect of magnetic nanoparticles of Fe3O4 and 5-bromotetrandrine on reversal of multidrug resistance in K562/A02 leukemic cells. *Int J Nanomedicine*. 2009;4:209–216.
13. Wang C, Zhang H, Chen B, Yin H, Wang W. Study of the enhanced anticancer efficacy of gambogic acid on Capan-1 pancreatic cancer cells when mediated via magnetic Fe3O4 nanoparticles. *Int J Nanomedicine*. 2011;6:1929–1935.
14. Zhang G, Ding L, Renegar R, et al. Hydroxycamptothecin-loaded Fe3O4 nanoparticles induce human lung cancer cell apoptosis through caspase-8 pathway activation and disrupt tight junctions. *Cancer Sci*. 2011;102(6):1216–1222.
15. Sato A, Tamura Y, Sato N, et al. Melanoma-targeted chemo-thermo-immuno (CTI)-therapy using N-propionyl-4-S-cysteaminylphenol-magnetite nanoparticles elicits CTL response via heat shock protein-peptide complex release. *Cancer Sci*. 2010;101(9): 1939–1946.
16. Kawai K, Li YS, Kasai H. Accurate measurement of 8-OH-dG and 8-OH-Gua in mouse DNA, urine and serum: effects of X-ray irradiation. *Genes and Environment*. 2007;29(3):107–114.
17. Galsky MD, Vogelzang NJ. Docetaxel-based combination therapy for castration-resistant prostate cancer. *Ann Oncol*. 2010;21(11): 2135–2144.
18. Harada M, Iwata C, Saito H, et al. NC-6301, a polymeric micelle rationally optimized for effective release of docetaxel, is potent but is less toxic than native docetaxel in vivo. *Int J Nanomedicine*. 2012;7: 2713–2727.
19. Ren Y, Zhang H, Chen B, et al. Multifunctional magnetic Fe3O4 nanoparticles combined with chemotherapy and hyperthermia to overcome multidrug resistance. *Int J Nanomedicine*. 2012;7:2261–2269.
20. Aljarrah K, Mhaidat NM, Al-Akhras MA, et al. Magnetic nanoparticles sensitize MCF-7 breast cancer cells to doxorubicin-induced apoptosis. *World J Surg Oncol*. 2012;10:62.
21. Karlsson HL, Cronholm P, Gustafsson J, Möller L. Copper oxide nanoparticles are highly toxic: a comparison between metal oxide nanoparticles and carbon nanotubes. *Chem Res Toxicol*. 2008;21(9):1726–1732.
22. Ma P, Luo Q, Chen J, et al. Intraperitoneal injection of magnetic Fe3O4-nanoparticle induces hepatic and renal tissue injury via oxidative stress in mice. *Int J Nanomedicine*. 2012;7:4809–4818.
23. Hussain SM, Hess KL, Gearhart JM, Geiss KT, Schlager JJ. In vitro toxicity of nanoparticles in BRL 3A rat liver cells. *Toxicol In Vitro*. 2005;19(7):975–983.
24. Naqvi S, Samim M, Abdin M, et al. Concentration-dependent toxicity of iron oxide nanoparticles mediated by increased oxidative stress. *Int J Nanomedicin*e. 2010;5:983–989.
25. Wang J, Yi J. Cancer cell killing via ROS: to increase or decrease, that is the question. *Cancer Biol Ther*. 2008;7(12):1875–1884.
26. Chen Y, Wang J, Fraig MM, et al. Defects of DNA mismatch repair in human prostate cancer. *Cancer Res*. 2001;61(10):4112–4121.
27. Trzeciak AR, Nyaga SG, Jaruga P, Lohani A, Dizdaroglu M, Evans MK. Cellular repair of oxidatively induced DNA base lesions is defective in prostate cancer cell lines, PC-3 and DU-145. *Carcinogenesis*. 2004;25(8):1359–1370.
28. Chaiswing L, Bourdeau-Heller JM, Zhong W, Oberley TD. Characterization of redox state of two human prostate carcinoma cell lines with different degrees of aggressiveness. *Free Radic Biol Med*. 2007; 43(2):202–215.
29. Gasparian AV, Guryanova OA, Chebotaev DV, Shishkin AA, Yemelyanov AY, Budunova IV. Targeting transcription factor NFkappaB: comparative analysis of proteasome and IKK inhibitors. *Cell Cycle.* 2009;8(10):1559–1566.
30. Jain G, Cronauer MV, Schrader M, Möller P, Marienfeld RB. NF-κB signaling in prostate cancer: a promising therapeutic target*? World J Urol*. 2012;30(3):303–310.
31. Koumakpayi IH, Le Page C, Mes-Masson AM, Saad F. Hierarchical clustering of immunohistochemical analysis of the activated ErbB/PI3K/Akt/NF-kappaB signalling pathway and prognostic significance in prostate cancer. *Br J Cancer*. 2010;102(7):1163–1173.
32. MacKenzie L, McCall P, Hatziieremia S, et al. Nuclear factor κB predicts poor outcome in patients with hormone-naive prostate cancer with high nuclear androgen receptor. *Hum Pathol*. 2012;43(9):1491–1500.
33. Jing H, Wang J, Yang P, Ke X, Xia G, Chen B. Magnetic Fe3O4 nanoparticles and chemotherapy agents interact synergistically to induce apoptosis in lymphoma cells. *Int J Nanomedicine*. 2010;5:999–1004.
34. Marano F, Hussain S, Rodrigues-Lima F, Baeza-Squiban A, Boland S. Nanoparticles: molecular targets and cell signalling. *Arch Toxicol*. 2011;85(7):733–741.